

Consideration for Use of an Inkjet Technology for Fabrication of Microwave Circuits

Veljko Napijalo, Dragana Vasiljević, Andrea Marić and Goran Stojanović

Abstract – The paper presents characterization of an Inkjet conductor printing technology utilizing silver conductive ink on flexible Kapton substrate for microwave applications. Microstrip ring resonator method has been used for measurement in the frequency band up to 20 GHz. Specific details related to application of the chosen method along with limitations of a technology on hand are provided. Results of the measurements suggest that the technology can not be used at microwave frequencies due to very low value of Q factor of the resonances and prohibitively high value of insertion loss. Measures to reduce losses have been proposed including the increase of conductor thickness and the increase of substrate thickness.

Keywords – Ink-jet technology, Flexible circuits, Microwave applications, Microwave measurements, Microstrip ring resonator.

I. INTRODUCTION

Modern applications of microwave circuits are currently being expanding from traditional, highly sophisticated and performance demanding areas, such as space, military or professional telecommunications, to areas like personal commodities, entertainment, and gaming. For an example, personal items like clothing and footwear, seamlessly equipped with various electronic circuits are turning into smart devices or systems, medical diagnostics aids or sensor networks. For these applications, in contrast to the traditional ones, the most important aspect to consider is the utilization of unconventional fabrication technologies to realize various microwave circuits and systems. The unconventional technologies must be compatible with core fabrication process and allow the realization of required functionality with minimal impact on the price. Typical examples of utilization of some unconventional fabrication techniques are antennas realized on textile substrates [1]-[2], multilayer microwave filter printed on paper substrate using conductive silver ink [3], and wideband ink-jet printed hybrid [4].

Special focus of the researchers is currently been addressed to microwave circuits on flexible substrates, which are basically made from polymers. It is driven by the vision that utilization of polymers as microwave circuit substrates [5]-[6], combined with ink-jet conductor printing, can potentially lead to excellent set of characteristics. The attractive characteristics are spanning from capability to conform with a desired shape to cost effectiveness and conformance with environment friendly initiatives. The later is due to the fact that traditional

fabrication processes are subtractive (tiny conductor pattern is obtained by removing substantial portion from solid metalized surface using toxic chemicals), while printing processes are additive (metal is printed on a surface only where needed) which reduces the cost and environment pollution.

This paper presents an expanded version of previously published work [8]. The paper present a characterization procedure carried out in order to determine the properties of an ink-jet conductor printing technology and address its suitability for realization of microwave circuits. Available printing equipment and processes which can, among many other possibilities, be used to print silver conductors on Kapton polymer flexible substrates, are available at the Faculty of Technical Sciences, University of Novi Sad.

The characterization process described in this paper is basically a description of a measurement procedure and analysis of the results carried out to determine or roughly estimate electrical and other important properties of dielectrics and conductors used for circuit fabrication. The measurement method is based on measurements of multiple resonances of the microstrip ring resonator [8]. A resonance occurs at each frequency where the perimeter of the ring equals a integer multiple of a wavelength. Multiple resonances of the resonator allow the calculation of relative dielectric constant and quality (Q) factor values in a wide frequency band. After these parameters have been determined, the technology would be sufficiently characterized for reliable design of microwave circuits. Results of the measurements of two simple filter circuits fabricated to verify the calculated values and the related conclusions are also presented.

II. SOME DETAILS RELATED TO UTILIZATION OF A RING RESONATOR

The frequency band, sufficiently wide to draw preliminary conclusions for this investigation has been found to be 20 GHz. A diameter or the ring resonator has been determined as a trade-off between area occupied by the resonator and a number of resonances in the frequency band of interest. A large quantity of silver ink must be used to fabricate microstrip ground plane. Therefore, it is important to reduce resonator area, which translates into minimal resonator diameter. On the other hand, resonant frequency is inversely proportional to the resonator diameter, so a reduction in diameter will cause a shift of the first resonance to higher frequency and will result in fewer resonances within the desired frequency band of 20 GHz. As a good trade-off, a first resonant frequency has been set to 2 GHz. Using *TxLine* [8], a resonator radius value of 14.85 mm has been found for a substrate height h of 125 μm . The corresponding medium

V. Napijalo, D. Vasiljević, A. Marić, and G. Stojanović are with Faculty of Technical Sciences, University of Novi Sad, Trg Dositeja Obradovića 6, 21000 Novi Sad, Serbia, E-mail: [napijalo, amaric, sgoran]@uns.ac.rs, dragana.vasiljevic87@gmail.com

length l of the resonator was 93.305 mm. Using the same program, a width of a microstrip line with a characteristic impedance of 50Ω w_{50} has been found to be approximately $300 \mu\text{m}$. A value of relative dielectric constant of Kapton substrate ($\epsilon_r=3.2$) used in the calculations has been taken from the data supplied by a manufacturer. The thickness t of silver printed conductors was $0.5 \mu\text{m}$.

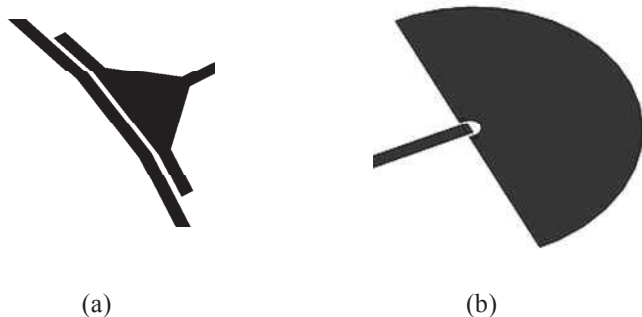


Fig. 1. Resonator details. (a) Detail of the enhanced periphery coupling. (b) Viasless coplanar waveguide-microstrip transition

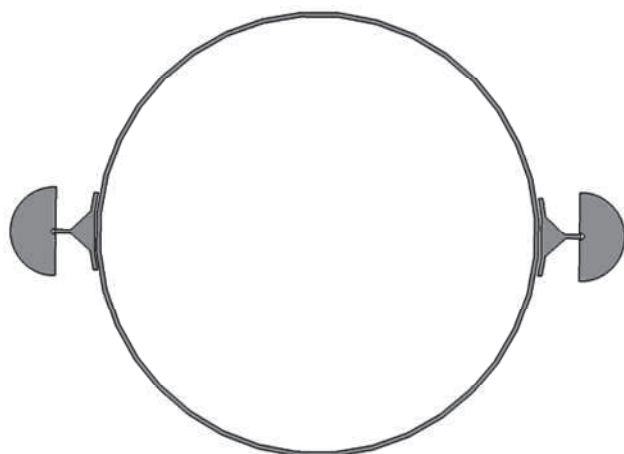


Fig. 2. Complete microstrip ring resonator circuit used for measurements

In order to perform measurements using a vector network analyzer and a probe station, it has been necessary to couple a resonator to external microstrip lines and to provide appropriate probe landing pattern. The coupling should be sufficiently strong to reliably measure the transmission coefficient of the resonator within the desired frequency band, but, on the other hand, not too strong to introduce distortion of the current distribution along the ring, as this can introduce measurement errors. It is convenient to choose the coupling in such a way that the transmission maxima are within the range of -20 dB to -40 dB [8]. It is possible to work with higher values, but in this case calculation of the unloaded quality factor, Q_0 , needs to be calculated from the values of the loaded quality factor Q_L and the values of the transmission S parameters at the resonances, which require very precise magnitude measurements. Various arrangements to couple the resonator to external microstrip lines are presented in [8]. For the particular case described in this paper, the most suitable method of coupling has been found to be the so-called

enhanced periphery which has been modified by adding a triangular taper to give required coupling values. The decisive factors to make such a choice have been related to technology limitations in reliable printing of conductor patterns. In particular, the minimum line width and minimal clearance between the conductors were $100 \mu\text{m}$. A value of the minimum clearance has been found to be too large to implement the simplest coupling arrangement possible i.e. to use open-end capacitance of the microstrip lines [8]. The optimized arrangement of the implemented enhanced periphery structure obtained using electromagnetic (EM) simulations is presented in Fig. 1 (a).

Similarly to the case of the resonator coupling, for the most convenient transition from coplanar ground-signal-ground (G-S-G) probes to a microstrip line, the technology must allow the use of plated through holes - vias [10]. As the current technology is not capable to provide vias, a suitable viasless transitions from [10] has been used. The transition utilizes a radial stub to provide a capacitance between ground tips of the probe and microstrip ground plane which effectively connect the grounds for a microwave signal. The structure of the transition presented in Fig. 1 (b) has been EM simulated and optimized using *Sonnet* [11]. The optimized outer radius of the stub was 3 mm. The dimensions from the inner side of the transitions have been determined to conform with dimensions required by a probe used - $250 \mu\text{m}$ gap between the signal and ground conductors. The whole resonator structure measured with a network analyzer is presented in Fig. 2.

III. RESULTS OF THE RING RESONATOR MEASUREMENTS

Test sample has been fabricated using Dimatix DMP-3000 ink-jet printer. S parameter measurements have been carried out using Agilent N5230A vector network analyzer and a probe station from SUS MicroTec. Measured values of S_{21} are presented in Fig. 3. The S parameter has unusual shape at the first resonance (around 2 GHz), so it can not be used for calculations. At all of the other resonances shape of the transmission S parameter is regular meaning that the influence of the discontinuities can be neglected, there is no significant distortion of the electromagnetic field and degenerate modes are not excited.

Values of Q factors of the resonances, which can be estimated from the transmission curve shown on Fig. 3, are considerably lower than values obtained using electromagnetic simulations assuming a value of conductivity for bulk silver ($\sigma=6.17 \cdot 10^7 \text{ S/m}$). A curve calculated using a value of conductivity of $\sigma=1.8 \cdot 10^7 \text{ S/m}$ is also shown in Fig. 3. This value provides approximately the same Q factors for the resonances and is in compliance with a ratio between conductivities of bulk and printed copper presented in [12]. As the electromagnetic simulations of the resonator structure shown in Fig. 2 are very time consuming due to multiple resonances, the fine tuning of printed conductors conductivity is impractical. Therefore, the rough estimation based on similar values obtained for Q factors can be adopted as initial conductivity value.

Effective dielectric constant can be calculated from measured resonant frequencies with the formula [8]:

$$\epsilon_{eff} = \left(\frac{nc}{2\pi fr} \right)^2 \quad (1)$$

where n is a number of the resonance, c is velocity of light in vacuum, f is measured resonance frequency which corresponds to n , and r is resonator radius. Loaded Q factor, Q_L can be determined from the expression:

$$Q_L = \frac{\omega_0}{\omega_u - \omega_l} \quad (2)$$

where ω_0 is a angular resonant frequency, ω_u and ω_l are angular frequencies corresponding to upper and lower frequencies of 3-dB transmission bandwidth around ω_0 . Unloaded Q factor, Q_0 , is calculated from:

$$Q_0 = \frac{Q_L}{1 - 10^{-IL/20}} \quad (3)$$

where IL is a value (expressed in dB) of the transmission S parameter (S_{21}) at the resonance. Determination of the Q factors has been performed using microwave CAD program [13]. Measured S parameter file have been read into the program, and frequencies f_0 , f_u and f_l have been determined for all of the resonant frequencies by placing markers at local transmission maxima at the resonance (f_0), and then placing additional markers to 3 dB lower magnitudes on both sides of the resonance (f_u and f_l). The process is illustrated in Fig. 4.

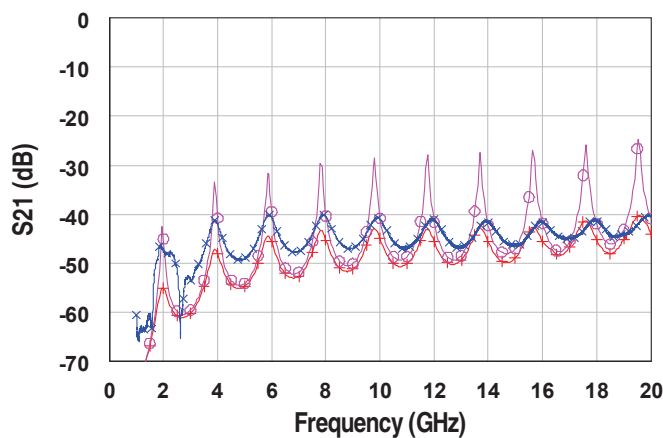


Fig. 3. S_{21} of the resonator structure from Fig. 2: -x- - measured results; -o- - EM simulated with $\sigma=6.17 \cdot 10^7$ S/m; -+- - EM simulated with $\sigma=1.8 \cdot 10^7$ S/m

Calculated values of effective dielectric constant ϵ_{eff} can be used to calculate relative dielectric constant ϵ_r of Kapton substrate at each resonant frequency. Calculations have been carried out using closed-form expressions for calculation of

microstrip effective dielectric constant from substrate and conductor dimensions, and material properties (including ϵ_r). These relations are built-in feature available in [8] and have been used here in an inverse fashion. For a given resonance frequency, a value of ϵ_r (which is an input parameter for direct calculation) has been varied until a value obtained for ϵ_{eff} within the program (an output parameter in direct calculation) would have coincide with a valued calculated based on Eq. (1). In such a manner, a input-output parameter relation has been reversed. Beside the agreement between ϵ_{eff} values calculated by [9] and obtained from Eq. (1), a value of ϵ_r can be additionally checked using other output data from [9]. As the program calculates a value for an electrical length for a given physical length of the conductor, for sufficiently accurate value of ϵ_r , the resonator length of 93.305 mm must be approximately equal to an electrical length of $n \times 360^\circ$ where n is the order of the resonance.

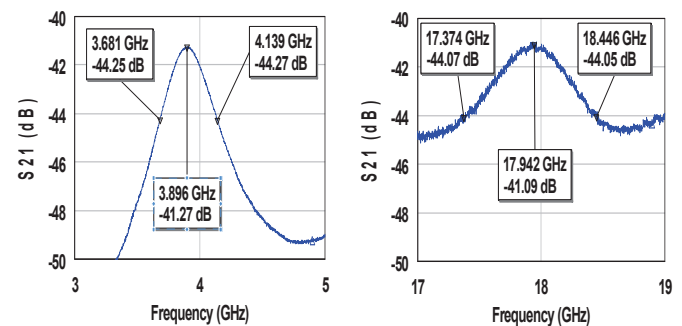


Fig. 4. Examples of determination of f_0 , f_u and f_l from measured S_{21} using options available in [13] for the 2nd and the 9th resonance

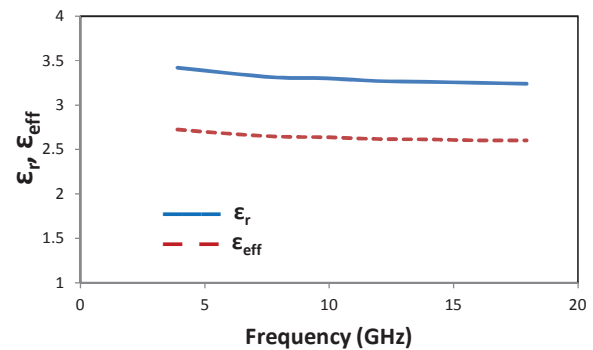


Fig. 5. Calculated values of ϵ_r and ϵ_{eff}

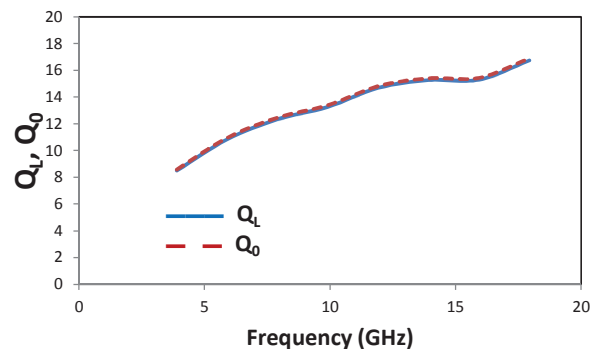


Fig. 6. Calculated values of Q_0 and Q_L

Calculated values for ϵ_r and ϵ_{eff} are presented in Fig. 5. At lower frequencies, a value for relative dielectric constant is higher than a value of $\epsilon_r=3.2$ given by the manufacturer. Values are decreasing with increasing a frequency and are within the range of 3.42 at 4 GHz to 3.27 at 12 GHz, decreasing very slowly to a value of 3.24 at 18 GHz.

Calculated values of Q_0 and Q_L are shown in Fig. 6. Values of the quality factors are very similar indicated that resonator loading during the measurements is minimal and can be neglected. Both quality factors are increasing with frequency, but values in the whole frequency band of interest remain very low spanning from 8.6 at lower frequencies to 17.9 at higher. Increase of quality factors with frequency is very unusual and will be explained in Section 5.

IV. RESULTS OF THE DC BLOCKING FILTERS MEASUREMENTS

Together with the ring resonator circuit from Fig. 2, test circuit of two DC blocking filters, a wideband and a narrowband, both with parallel coupled microstrip lines, have been fabricated. The central operating frequency of the filters was around 6.5 GHz. The filters have been designed using EM simulations [11]. In the simulations, the conductors have been approximated as perfect (lossless), zero thickness metal. The relative dielectric constant value has been set to $\epsilon_r = 3.2$. The motivation for realization of such simple test circuit within the scope of characterization of the ink-jet technology on hand was to test the validity of the calculated value of ϵ_r .



Fig. 7. Wideband microstrip DC block filter layout

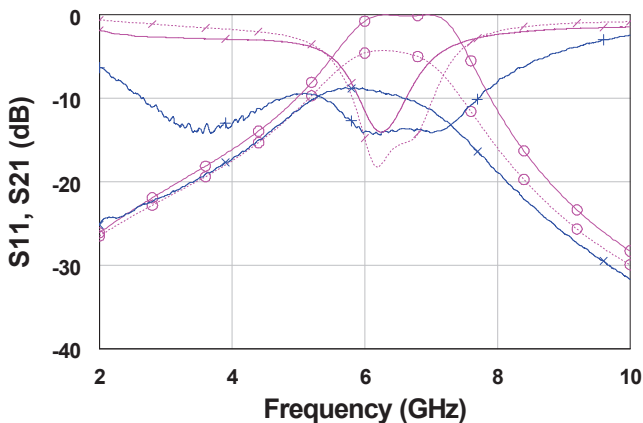


Fig. 8. S parameters of wideband microstrip DC block filter from Fig. 7: -x- – measured S_{21} ; +- – measured S_{11} ; -o- – EM simulated S_{21} ; -/- – EM simulated S_{11} . EM simulations with $\epsilon_r=3.36$ and $\sigma=1.8 \cdot 10^7$ S/m are displayed with dotted lines

The layout of the wideband filter is presented in Fig. 7. Measured S parameters of the filter and the results of EM simulations are shown in Fig. 8. The measured insertion loss of the filter is very high, approximately 10 dB at the central frequency indicating high loss of the conductors. For the same reason, the reflections (S_{11}) outside the passband are reduced indicating that reflected waves are significantly attenuated. Central operating frequency is shifted downwards to 6.062 GHz. The filter circuit has been EM re-simulated using a previously calculated value for relative dielectric constant of Kapton substrate of $\epsilon_r=3.36$, estimated value for conductivity of printed silver of $\sigma=1.8 \cdot 10^7$ S/m for both, signal conductor and a ground plane, and with finite signal conductor thickness of $t=0.5 \mu\text{m}$. Values of S parameters after re-simulation are also shown in Fig. 8 with dotted lines.

The layout of the narrowband filter is illustrated in Fig. 9 while the measured and EM simulated S parameters are presented in Fig. 10. The narrowband filter also has a high value of the insertion loss of approximately 11 dB at the central frequency and the reduced values of reflections outside the passband. Poor performance is again due to high conductor losses. Re-simulated values, which take into account values of ϵ_r and σ , are in much better agreement with measured results than in the case of the wideband filter.



Fig. 9. Narrowband microstrip DC block filter layout

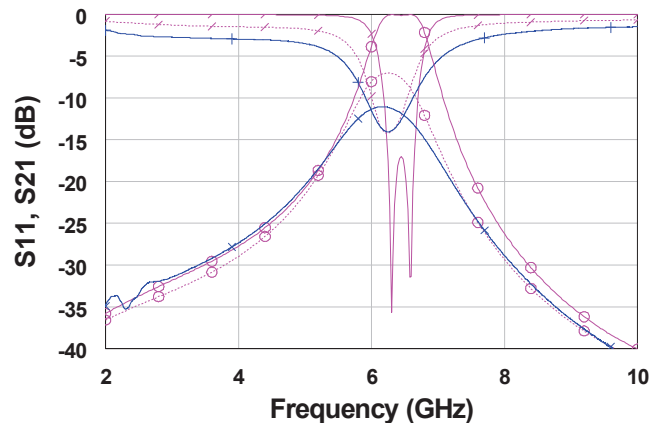


Fig. 10. S parameters of narrowband microstrip DC block filter from Fig. 9: -x- – measured S_{21} ; +- – measured S_{11} ; -o- – EM simulated S_{21} ; -/- – EM simulated S_{11} . EM simulations with $\epsilon_r=3.36$ and $\sigma=1.8 \cdot 10^7$ S/m are displayed with dotted lines

V. ANALYSIS OF RESULTS AND SUGGESTIONS FOR IMPROVEMENT

Analyzing the results of EM re-simulations presented in Figs. 8 and 10, it can be concluded that a value of relative

dielectric constant has been determined with good accuracy, as the agreement between central operating frequency of the filters is in much better agreement than when a value from a datasheet is used.

For the case of the wideband filter from Fig. 7, the remaining difference between EM re-simulated and measured central frequency of 372 MHz (5.8 %) in Fig. 8 can be explained by another limitation of the technology. The wideband filter structure from Fig. 7 uses microstrip coupled line arrangement with line width/spacing of 100 μm /100 μm . These are the minimal recommended values, which means that a line will not brake providing it has at least a minimum width, and that the two lines will not touch each other providing they are separated at least by minimal clearance. In the case where a dimension is set to a recommended minimum, conductor pattern will typically be fabricated with large relative tolerances. The DC blocking filter circuit is particularly sensitive to the tolerances and tends to shift downwards in frequency if coupled conductor widths are narrower than a nominal value of 100 μm , and/or if the spacing between them is wider than 100 μm , which explains the disagreement still present in Fig. 8. The narrowband filter structure from Fig. 9 is composed of a coupled line section with line width/spacing values of 200 μm /200 μm respectively, which is far away from minimal recommended values. Accordingly, the narrowband filter is less sensitive to fabrication tolerances which results in an excellent agreement between measured and re-simulated central operating frequencies in Fig. 10 (82 MHz - 1.3 %).

The influence of estimated value for σ to bring the re-simulated values of S parameters closer to measured ones is qualitatively confirmed as well. The trend of decreasing values of reflections outside the passband and increasing the insertion loss is illustrated in Fig. 8. However, the values of measured and re-simulated values are still very far. It will be explained that this discrepancy can result from some other causes apart from σ value.

TABLE I
THE ANALYSIS OF LOSSES FOR 50 Ω LINES AT 8 GHz

h (μm)	125	125	125	125	300
$w_{50\Omega}$ (μm)	300	300	300	300	700
t (μm)	0.5	20	0.5	20	0.5
σ (10^7 S/m)	6.17	6.17	1.8	1.8	1.8
L (dB/m)	14.5	7.6	40.1	13.6	17.2
L_λ (dB/ λ)	0.36	0.19	1.0	0.34	0.42

Values of σ are typically determined from DC resistance measurements of a very long conductor which has been impossible to carry out due to practical reasons. Besides, the separation of microstrip losses to dielectric and conductor losses (when radiation losses are negligible) is possible only where σ value is known. Therefore, the separation of losses has not been carried out, but this does not affect the significance of this work as it will be shown that conductor losses are by far dominant for the particular case of the technology on hand.

Values of per-unit-length attenuation L and values normalized to a wavelength L_λ at 8 GHz for several illustrative cases of 50 Ω microstrip lines using silver conductors are presented in Table I. The values have been calculated using another built-in feature from [9]. It can be concluded that even for the case of bulk silver conductors with 0.5 μm thickness, a value of attenuation is relatively high having in mind that silver is the best conductive material available. Nonetheless, a value of $L_\lambda=0.36$ dB/ λ can be considered as acceptable for the context of applications described in the introduction. Increasing the conductor thickness to 20 μm results in the attenuation reduction of approximately two times for the conductors made of bulk silver, and approximately three times for printed conductors. Therefore, besides the significantly reduced conductivity of the printed silver conductors, a thickness of the conductor of 0.5 μm is also responsible for the low value of the quality factor of the resonator and the high value of the insertion loss of the DC blocking filters. Increasing the thickness of printed silver conductors to a value of 20 μm will result in a value of per-unit-length attenuation approximately equal to a value obtained for conductors made from bulk silver with 0.5 μm thickness. In other words, it would become acceptable for the realization of microwave circuits. However, such an approach is not feasible with the particular ink-jet printing technology as it requires the process of conductor printing to be repeated forty times!

Another possible approach to reduce the attenuation would be to increase the thickness of the Kapton substrate, e.g. from 125 μm to 300 μm . This will result in increased conductor width for a 50 Ω line. Increased width, even for the case of printed silver thickness of 0.5 μm , results in an acceptable attenuation. On the other hand, it is important to keep the substrate thickness at reasonable values to conform with the basic motives for ink-jet technology implementation in the scope of this paper, the flexibility of the fabricated circuits.

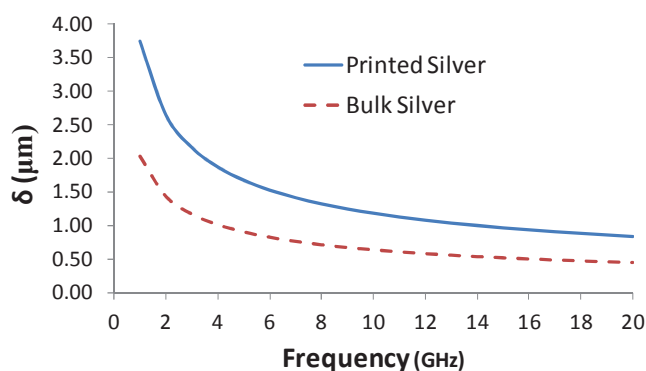


Fig. 11. Skin depth as a function of frequency for printed and bulk silver

Contribution of losses in microstrip ground plane have not been taken into account in previous analysis as they are not included in the closed-form expressions contained in [9]. Besides ohmic losses, the mechanism of the ground plane contribution to overall attenuation possibly includes radiation

losses as a thin printed conductor represents a poor shield for electromagnetic field due to the ratio between skin depth δ and conductor thickness t . The skin depth δ for conductors made from bulk and printed silver as a function of frequency is presented in Fig. 11. Formula from [14] has been used for the calculations of δ values. At lower frequencies the skin depth is considerably larger than conductor thickness. As the frequency increases, a value for the skin depth approaches a value of conductor thickness and the effectiveness of the shield is improving. This is perhaps the only way to explain the unusual increase in quality factors with frequency shown in Fig. 6. Besides that, it becomes apparent that the loss analysis must include radiation losses which are in this particular case of unusual cause as they are not coming from strip radiation, but rather from imperfect ground plane.

The visual inspection of the printed conductors has revealed imperfections like surface roughness and edge ripples of microstrip signal conductors. It is well known that such imperfections could influence a value of total conductor loss and must be eliminated or taken into account in future work.

The analysis carried out illustrates that a balance should be found between amounts of simultaneous increase of the thickness of printed silver conductors and increase of the substrate thickness. The practical side must be considered, i.e. a number of repeated printings and a degree of the flexibility of Kapton substrate after increasing the thickness. It is clear that the optimum solution can be found and that a modified ink-jet technology could be used to fabricate microwave circuits for previously described, unconventional applications.

VI. CONCLUSION

A procedure carried out in order to characterize a ink-jet conductor printing technology for microwave circuit realization together with measured and calculated results has been presented in this paper.

Measurement of a transmission S parameter of a microstrip ring resonator has been adopted and all specific details related to the particular implementation of the method along with the technology on hand have been described.

The calculated values of Q factors are very low and insertion losses of the test filter circuits are very high. These indicate that the losses of the conductors made of printed silver are prohibitively high for microwave circuits applications. Besides the conductivity of the printed silver conductors being much lower than the conductivity of bulk silver, the very small conductor thickness plays an important role in causing high losses. A trade-off between utilization of thicker conductors and thicker Kapton substrate, as both of the actions tend to reduce losses, can be found, but attention to practical aspects must be exercised.

For more versatile microwave applications, it is of crucial importance to upgrade the technology to include via making capabilities as without the upgrade the technology will remain limited to a very specific class of circuits. Upgrade can be made in conformance with the printing process as a substances required to etch away holes in Kapton substrate are available as inks for the same printing equipment. It is also

feasible to print some adhesive materials and extend a range of applications to include multilayer microwave circuits, which represent a very attractive topic for research and implementation within microwave community. Furthermore, to achieve better control of the conductor dimensions and improve regularity of their shape, both leading to improved printing resolution, substrate surface treatment can be considered.

It is clear that a potential to implement an ink-jet printing technology to fabrication of microwave circuits is huge, and that motivation and possibilities for future research are enormous.

ACKNOWLEDGEMENT

This paper has been resulted from research activities of research team at the Faculty of Technical Sciences, University of Novi Sad within the scope of the project TR32016 and FP7 project APOSTILLE, no. 256615.

REFERENCES

- [1] V. K. Palukuru, A. Pekonen, V. Pznttari, R. Makinen, J. Hagberg and H. Jantunen, "An Inkjet-Printed Inverted-F Antenna for 2.4GHz-Wrist Application," *Microw. Opt. Technol. Lett.*, vol. 51, no. 2, pp. 2936-2938, Dec, 2009.
- [2] S.-J Ha, Z. -B. Jung, D. H. Kim and C. W. Jung, "Textile Patch Antennas Using Double Layer Fabrics for Wrist-Wearable Applications," *Microw. Opt. Technol. Lett.*, vol. 54, no. 12, pp. 2697-2702, Dec, 2012.
- [3] L. Zang, A. Rida, R. Vyas and M. M. Tentzeris, "RFID Tag and RF Structures on a Paper Substrate Using Inkjet-Printing Technology," *IEEE Trans. Microw. Theory Techn.*, vol. 55, no. 12, pp. 2894-2901, Dec, 2007.
- [4] W. Arriola, M. Lee, Z. Kim, E. Rzu and I. S. Kim, "New Inkjet Printed Wideband 3 dB Branch Line Coupler," *IEEE MTT-S Int. Microw. Symp. Dig.*, Baltimore, USA, pp. 1-4, 5-10 June, 2011.
- [5] M. Swaminathan, V. Sundaram, J. Papapolymerou and P. M. Raj, "Polymers for RF Apps," *IEEE. Microw. Magazine*, vol. 12, no. 7, pp. 62-77, Dec, 2011.
- [6] A. -V. Pham, "Packaging with Liquid Crystal Polymer," *IEEE. Microw. Magazine*, vol. 12, no. 5, pp. 83-91, Aug, 2011.
- [7] K. Chang and L.-H. Hsieh, *Microwave Ring Circuits and Related Structures*, 2nd ed. Hoboken, USA: Wiley, 2004.
- [8] V. Napijalo, D. Vasiljević, A. Marić and G. Stojanović, *Characterization of Microwave Structures Fabricated Using Inkjet Technology*, LVII ETRAN. Zlatibor, Serbia, paper MT 2.1, 2013 (in Serbian).
- [9] TxLine, AWR Corporation, El Segundo, CA, USA
- [10] R. N. Simons, *Coplanar Waveguide Circuits, Components and Systems*, New York, USA: Wiley, 2001.
- [11] Sonnet. ver. 12.52, Sonnet Softw., North Syracuse, NY, 2009.
- [12] J. S. Kang, H. S. K. J. Ryu, H. T. Hah, S. Jang and J. W. Joung, "Inkjet Printed Electronics Using Copper Nanoparticle Ink," *J Mater Sci: Mater Electron*, vol. 21, pp. 1213-1220, 2010.
- [13] *Microwave Office*, ver. 9.0, AWR Corporation, El Segundo, CA, USA
- [14] B. C. Wadell, *Transmission Line Design Handbook*, Boston, MA, USA: Artech House, 1991.